# Terahertz Imaging With Quantum-Cascade Laser and Quantum-Well Photodetector

Z. Y. Tan, Tao Zhou, J. C. Cao, and H. C. Liu, *Fellow, IEEE*

*Abstract*— A transmission imaging system based on a terahertz quantum-cascade laser and a spectrally-matched quantum-well photodetector is presented. Terahertz imaging of paper money is demonstrated. An imaging resolution of 0.5 mm is achieved. This experiment demonstrates that the laser and the photodetector are potentially useful for imaging applications.

*Index Terms*— Terahertz, imaging, quantum-cascade laser, quantum-well photodetector.

## I. INTRODUCTION

TERAHERTZ (THz) imaging is a promising technology for applications in security screening, biomedical imaging, active remote sensing, and material characterizations [1], [2]. The first demonstration of terahertz imaging of a circuit and a leaf was realized by employing an optically gated terahertz transmitter and a corresponding detector [3]. After that, research on imaging with terahertz radiation had been rapidly developed in the past ten years [4]–[8]. The terahertz quantum-cascade laser (QCL) [9] is one of the important terahertz solid-state sources with high output power and compact structure. Experiments on biological tissues and real-time imaging for fingerprint identification were demonstrated by using terahertz QCLs as light sources [10]–[12]. However, the terahertz detectors used in these systems were thermal detectors with slow response of about ten milliseconds. The terahertz quantum-well photodetector (QWP) [13], [14] is one of the promising detectors with fast response time and can spectrally match the terahertz QCL. It has been used in characterizing thermal quenching of terahertz QCLs [15] and in passive terahertz imaging [16]. However, the the signal-to-noise (SNR) is not high in this passive imaging demonstration.
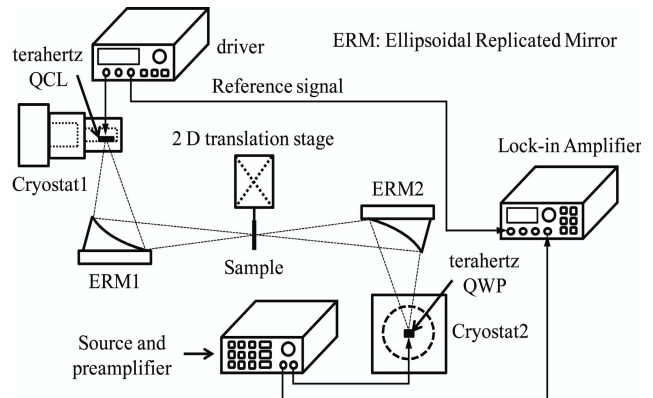
Fig. 1. Schematic of the set-up for terahertz transmission imaging.

In order to obtain a good SNR in imaging, in this letter, a terahertz QCL as a light source is employed. A transmission imaging setup is built by employing a terahertz QCL, a spectrally- matched QWP, two Ellipsoidal Replicated Mirrors (ERMs for short), and a two-dimensional translation stage. The terahertz light beam spot at the confocal point of two ERMs is acquired and analyzed. The terahertz transmission image of the watermark of a paper money is acquired. The imaging resolution is analyzed and discussed.

## II. EXPERIMENTAL SETUP

The terahertz light source in our experimental setup is a GaAs/AlGaAs-based terahertz QCL, with an active region consisting of three-well modules [17], [18], emitting at 3.90 THz. The terahertz QCL, operating at 11 K, is fixed to a copper heat sink and mounted onto the cold finger of a closed-cycle helium cryostat (Cryostat1) with a cooling power of about 2.2 W at 10 K. The light receiver is a GaAs/AlGaAs-based terahertz QWP (v267) [14] with a size of 0.8 mm × 0.8 mm. The QWP is cooled down to 3.2 K by a closed-cycle helium cryostat (Cryostat2) with a low temperature limit of 2.8 K. The peak response frequency of the detector is 3.22 THz with a responsivity of about 0.5 A/W and a detectivity of about $10^{11}$ cm·Hz$^{1/2}$/W [14].

A schematic of the experimental setup is shown in Fig. 1. The sample is placed at the focal plane (X-Y plane) of two ERMs both with a long focal length of 183 mm and mounted on a computer controlled X-Y translation stage. The terahertz QCL is driven by a high power pulse generator. The driving voltage is 13 V with a frequency of 20 Hz. The emitted terahertz light from QCL is collected by the ERMs and then focused onto the terahertz QWP. The signal current generated by the detector is extracted as a voltage by a low noise current preamplifier. The amplified voltage is read out by a lock-in
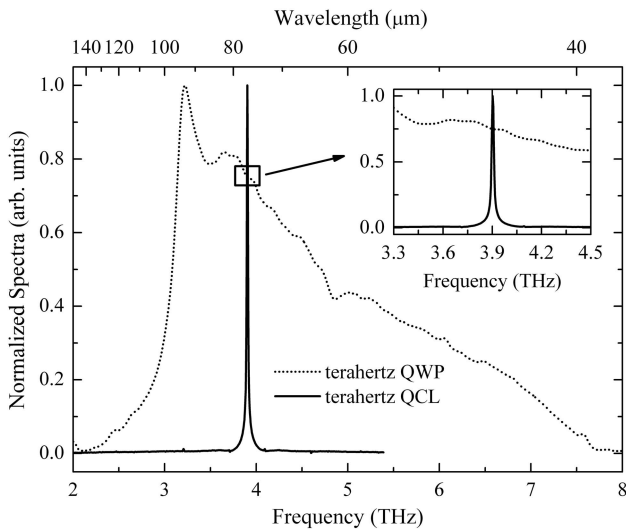
Fig. 2.    Normalized spectra of the terahertz laser emission and the detector response.



Fig. 3.    The dimension of the terahertz beam spot in X and Y directions measured by employing a sharp metallic blade.

amplifier (LIA) controlled by a computer for synchronization with the X-Y translation stage, and is displayed on the oscilloscope simultaneously. Normalized spectra of the laser emission and the detector response are compared in Fig. 2. From the inset, it is clear that the response of the detector is flat around the emission frequency (3.90 THz) of the laser. Therefore, as a receiver, the detector is well suited for this frequency point.

## III. RESULTS AND DISCUSSIONS

First, we evaluated the beam spot size of the laser in the sample plane using the knife-edge method [19]. A sharp metallic blade was placed in the confocal plane of the ERMs and moved along the X (horizontal) and Y (vertical) directions. The scan step of the blade is set to 0.125 mm in both directions. The measured results are shown in Fig. 3. According to the method used in Ref. [18], the effective size of the terahertz beam in each of the X and Y directions is approximately equal to the "clip width" of the beam measured in each of the two transverse dimensions. The clip levels used in this letter are in the range around 10% and 90% [19]. Therefore, the size of the beam spot is estimated to be 0.625 mm ($\Delta x$) and 0.813 mm ($\Delta y$) from the results shown in Fig. 3, where $\Delta x$ is $\Delta x = (\Delta x_1 + \Delta x_2)/2$, and $\Delta y$ is obtained by the same method. The large beam spot is due to the mechanical vibration of the closed-cycle helium cryostat. The amount of vibration is more in Y direction. Another important factor that influences the image quality is the SNR. The noise level due to the dark current of the detector was 2 mV. This gives a dynamic range of about 100:1 in our system, which is better than that in Ref. [16].

Next, a transmission image of the watermark of a paper money is collected. The scan step of the sample is set to 0.5 mm both in X and Y directions. Fig. 4(b) shows the resulting terahertz image from the watermark region of a paper money and Fig. 4(a) shows a comparison with its optical image (photograph). The size of the watermark region is
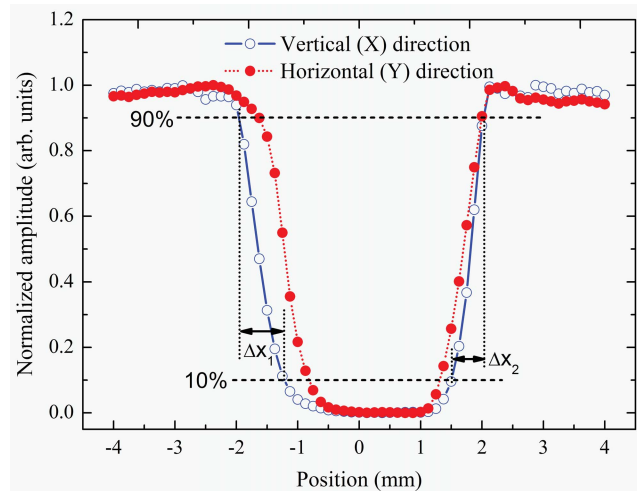
$33 \times 52$ mm$^2$ and the image consists of 7035 pixels with a spacing of 0.5 mm between neighboring pixels. The total scanning time takes about three hours. The speed is limited by the translation scan mechanism and the integration time, with a value of 300 ms, used in the LIA.

In the terahertz imaging, the portrait watermark area (barely visible in the optical image) is clearly shown. Different hair cluster in the head area can be clearly distinguished.

In order to estimate the spatial resolution of the terahertz image in Fig. 4(b), the transmission amplitude of a cross section at Y = 4.0 mm (the red short dashed line) in the image is drawn in Fig. 4(c). We choose half amplitude as a threshold to estimate the spatial resolution. The values of the signal above the blue short dashed line represent high transmission part in the paper money, displayed with nearly white color in Fig. 4(b). In Fig. 4(c), point A represents the transmission amplitude in the area of no pattern, and point B the area of pattern "1". The distance between point A and B represents the spatial resolution in the "100" pattern region which is estimated 0.5 mm from the intensity line. The distance between the points B and C represents the width of pattern "1" which is estimated 1.0 mm, and the real width on the paper money is about 1.5 mm. By the same method, in the "100" watermark area, because there is no scanning point between points D and E, the spatial resolution is less than 0.5 mm. The width of watermark "1" is estimated less than 1.0 mm, and the real value on the paper money is about 1.0 mm. Therefore, the best spatial resolution is about 0.5 mm in our experiments. The values of the signal below the blue dash-dotted line represent the low transmission part in the paper money, displayed with nearly black color. We can see five lower values below the short dot line, which corresponding to the five crossing points of the red short dashed line and the "100" pattern in Fig. 4(b).

The results acquired by employing our transmission imaging system provide a proof-of-concept demonstration, however the imaging resolution should be improved in further work. A liquid helium cryostat with nearly no vibration should be employed for the laser. Using a helium dewar in place of
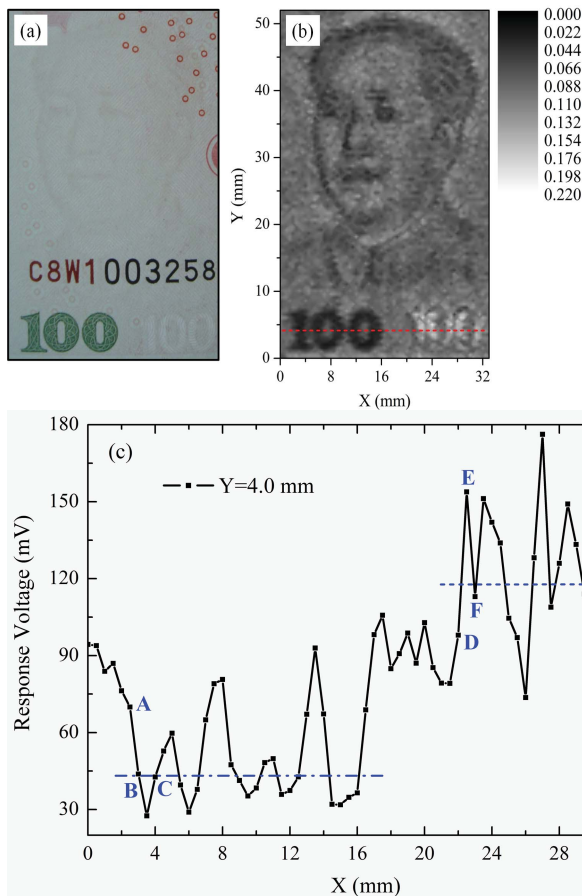
Fig. 4. Optical (a) and terahertz image (b) of the watermark region of a paper money. (c) The transmission amplitude of a cross section of the terahertz image in (b); the red short dashed line indicates the location Y = 4.0 mm.

closed-cycle mechanical cryostat to cool down the detector may also be a better choice. A faster mechanical scanning mechanism may be employed to shorten the imaging time in further work, such as the fast opto-mechanical scanning system. Meanwhile, further improvement in SNR and trade-off considerations between scan speed and integration time must be made.

## IV. CONCLUSION

We have demonstrated transmission imaging based on a terahertz QCL and a spectrally-matched QWP. A terahertz image of the watermark area of a paper money has been acquired. An imaging resolution of 0.5 mm has been obtained. The experiment has shown that the terahertz QCL and QWP devices are good candidates for transmission imaging. For

obtaining better resolution, low-vibration cryostats should be used for both the laser and the detector. To obtain a much shorter imaging time, a faster mechanical scanning mechanism may be used and the SNR of the system must be improved in further work.

## REFERENCES

[1] P. H. Siegel, "Terahertz technology," *IEEE Trans. Microw. Theory Tech.*, vol. 50, no. 3, pp. 910–928, Mar. 2002.

[2] M. Tonouchi, "Cutting-edge terahertz technology," *Nature Photon.*, vol. 1, pp. 97–105, Feb. 2007.

[3] B. B. Hu and M. C. Nuss, "Imaging with terahertz waves," *Opt. Lett.*, vol. 20, no. 16, pp. 1716–1718, Aug. 1995.

[4] Z. Jiang, X. G. Xu, and X.-C. Zhang, "Improvement of terahertz imaging with a dynamic subtraction technique," *Appl. Opt.*, vol. 39, pp. 2982–2987, Jun. 2000.

[5] R. M. Woodward, *et al.*, "Terahertz pulse imaging in reflection geometry of human skin cancer and skin tissue," *Phys. Med. Biol.*, vol. 47, no. 21, pp. 3853–3863, Oct. 2002.

[6] J. F. Federici, *et al.*, "THz imaging and sensing for security applications, explosives, weapons and drugs," *Semicond. Sci. Technol.*, vol. 20, pp. 5266–5280, Jun. 2005.

[7] W. L. Chan, J. Deibel, and D. Mittleman, "Imaging with terahertz radiation," *Rep. Progr. Phys.*, vol. 70, pp. 1325–1379, Jul. 2007.

[8] B. Recur, *et al.*, "Investigation on reconstruction methods applied to 3D terahertz computed tomography," *Opt. Express*, vol. 19, no. 6, pp. 5105–5117, Mar. 2011.

[9] R. Köhler, *et al.*, "Terahertz semiconductor-heterostructure laser," *Nature*, vol. 417, pp. 156–159, Feb. 2002.

[10] M. Beck, M. Giovannini, and J. Faist, "Imaging with a terahertz quantum cascade laser," *Opt. Express*, vol. 12, no. 9, pp. 1879–1884, May 2004.

[11] S. M. Kim, F. Hatami, and J. S. Harris, "Biomedical terahertz imaging with a quantum cascade laser," *Appl. Phys. Lett.*, vol. 88, no. 15, pp. 153903-1–153903-3, Apr. 2006.

[12] A. W. M. Lee, B. S. Williams, S. Kumar, Q. Hu, and J. L. Reno, "Real-time imaging using a 4.3-THz quantum cascade laser and a 320 × 240 microbolometer focal-plane array," *IEEE Photon. Technol. Lett.*, vol. 18, no. 13, pp. 1415–1417, Jul. 1, 2006.

[13] H. C. Liu, C. Y. Song, A. J. SpringThorpe, and J. C. Cao, "Tera-hertz quantum-well photodetector," *Appl. Phys. Lett.*, vol. 84, no. 20, pp. 4068–4070, May 2004.

[14] H. Luo, H. C. Liu, C. Y. Song, and Z. R. Wasilewski, "Background limited terahertz quantum-well photodetector," *Appl. Phys. Lett.*, vol. 86, pp. 231103-1–231103-3, Jun. 2005.

[15] S. Fathololoumi, *et al.*, "Time-resolved thermal quenching of THz quantum cascade lasers," *IEEE J. Quantum Electron.*, vol. 46, no. 3, pp. 396–404, Mar. 2010.

[16] T. Zhou, *et al.*, "Terahertz imaging with quantum-well photodetectors," *IEEE Photon. Technol. Lett.*, vol. 24, no. 13, pp. 1109–1111, Jul. 1, 2012.

[17] H. Luo, S. R. Laframboise, Z. R. Wasilewski, G. C. Aers, H. C. Liu, and J. C. Cao, "Terahertz quantum-cascade lasers based on a three-well active module," *Appl. Phys. Lett.*, vol. 90, pp. 041112-1–041112-3, Jan. 2007.

[18] S. Kumar, Q. Hu, and J. L. Reno, "186 K operation of terahertz quantum-cascade lasers based on a diagonal design," *Appl. Phys. Lett.*, vol. 94, pp. 131105-1–131105-3, Apr. 2009.

[19] A. E. Siegman, M. W. Sasnett, and T. F. Johnston, "Choice of clip levels for beam width measurements using knife-edge techniques," *IEEE J. Quantum Electron.*, vol. 27, no. 4, pp. 1098–1104, Apr. 1991.